Proceedings of the
47th IEEE Conference on Decision and Control
Cancun, Mexico, Dec. 9-11, 2008

Oscillatory Failure Case detection for new generation Airbus aircraft: a model-based challenge

Loïc Lavigne[1], Ali Zolghadri, Philippe Goupil and Pascal Simon

Abstract— **Robust and early detection of Oscillatory Failure Case (OFC) in the Electrical Flight Control System (EFCS) of new generation aircraft (A/C) appears to be a challenging problem. OFC leads to strong interactions with loads and aero-elasticity and consequently must be detected in time. A robust analytical redundancy-based technique implemented in A380 Flight Control Computer (FCC) is used for detecting such unauthorized oscillatory events. The technique has been successfully validated and provides a complete OFC coverage without false alarms in the A380 EFCS. However, for upcoming and future generation A/C, it could be required to detect OFC with less important amplitude. To meet this requirement, it becomes necessary to get more sensitive fault indicating signals. It is shown that the model quality can be significantly improved by reliable estimating of some physical parameters. The fault indicating signals obtained with the proposed methodology are compared to those obtained from A380 FCC during flight tests. The results are quite encouraging and suggest that OFC with less important amplitude could be successfully detected by the new strategy.**

I. Introduction

OFC results in an unwanted control surface oscillation, leading to strong interactions with loads and aero-elasticity when located within actuator bandwidth [12]. Consequently, OFC must be detected in time. Early and robust detection of OFC is very important because it has an impact on the structural design of the A/C. The model-based approach implemented in the A380 permits stringent requirements to be met with low computational cost [12]. This solution is currently used on in-service Airbus A380 to ensure OFC detection, providing a complete coverage of such events. However, for upcoming and future A/C, it could be required to detect OFC with less important amplitude in less time while keeping a good robustness. Since the precursor works of Jones [1] and Beard [2], many model-based FDI methods have been developed during the past decades. See for instance [3]-[7] for a survey. They offer many attractive features for improving the existing fault diagnosis techniques (see [3], [4], [9], [10], [12], [13]). However, to the best of our knowledge, model-based FDI techniques have not been used so far in on board A/C computers. The first reported work on oscillatory fault detection is [24], in which a set of methods called OFIS (Oscillatory Failure Identification System) was presented. The methods correspond to different fault situations (solid, liquid, …) and are based on a combination of linear methods and signal processing. In [25] a dynamic estimator with global convergence property is proposed to reconstruct the unknown values of an oscillatory signal. The design method is independent of the actuator's model. The convergence time is however relatively important, which makes the approach not suitable to OFC. In this paper, an attempt is made to present a complete and new methodology for robust detection of OFC. The modeling stage is based on on-line joint parameter/state estimation, allowing for model parameter variations during A/C flight. This modeling process is associated with the same decision making rules as currently used for in-service Airbus A380. The performance of the proposed fault detection scheme is measured by its detection delay, its propensity to issue false alarms and whether it permits a failure to go undetected. The performance indicators are assessed and discussed based on the simulation results. The data used in simulations correspond to real flight data provided by Airbus France, Toulouse. The work presented here describes the status of on going research activity undertaken within a collaborative research project which aims at providing a general framework in which various design goals and trades-off can be easily formulated and managed.

The paper is organized as follows. The OFC detection context is presented in section II. Section III is devoted to the description of the OFC detection strategy implemented on in-service A380. Section IV describes the proposed methodology. Section V discusses the results. Finally, some concluding remarks are given in a final section.

II. OFC failures: problem setting

EFCS, first developed by Aerospatiale and installed on Concorde (analogue system) and then designed with digital technology on Airbus A/C from the 80s (A310), provides more sophisticated control of the A/C and flight envelope protection functions [20],[21],[23]. In parallel, introduction of Fly By Wire (FBW) technology leaded to strong interactions between EFCS and flight physic disciplines, in particular interactions with loads and aero-elasticity. The study of these interactions leads to determine the OFC level to detect and the time allowed for the confirmation, for each control surface. Thus, it is required to be able to detect small amplitude OFC in a short delay.

The capability to detect these failures is very important because it has an impact on the structural design of the A/C. The load envelope constraints must be respected. More precisely, if OFC of given amplitude cannot be detected and passivated, this amplitude must be considered for load

Loic Lavigne, Ali Zolghadri, Pascal Simon, IMS-Automatic Control Department, 351 cours de la lmibération, 33405 Talence, France. loic.lavigne@laps.ims-bordeaux.fr. [1]Corresponding author.

Philippe Goupil is with AIRBUS France, Flight Control System – AIRBUS France – philippe.goupil@airbus.com

computations. If the result of this computation is too high, this can lead to reinforce the structure, degrading A/C performances. In order to avoid reinforcing the structure and consequently to gain weight, low amplitude OFC must be detectable quickly.

In this paper, only OFC located in the servo-loop control of the moving surfaces are considered, between the FCC and the control surface, including these two elements (Fig. 1). Consequently, the considered failure impacts only one control surface. OFC are mainly due to electronic components in fault mode generating spurious sinusoidal signals. This oscillatory signal propagates through the servo-loop control, leading to control surface oscillation. The faulty components are located inside the Analog Inputs/Outputs, the position sensors or the actuators. The FCC may also generate unwanted oscillations of the command current sent to the actuator servo-valve. OFC signals are considered as sinusoidal signals with frequency and amplitude uniformly distributed over the frequency range 0-10 Hz. Beyond 10 Hz, OFC have no significant effects because of the low-pass behavior of the actuator. It is necessary to detect OFC beyond a given amplitude in a given number of periods, whatever the OFC frequency. The time detection is expressed in period numbers, which means that, depending on the failure frequency, the time really allowed for detection is not the same.

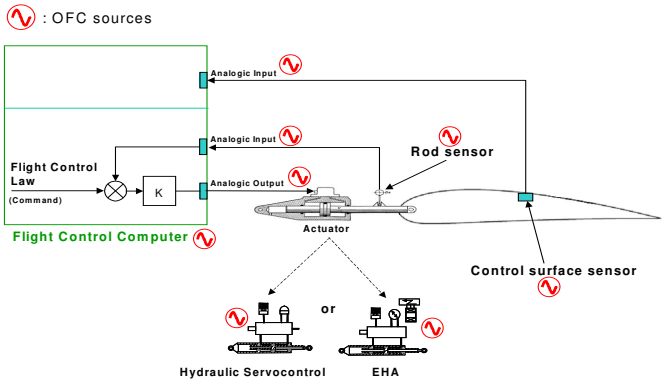

Fig. 1: OFC source localization in the servo-loop control of a control surface.

The main objective of this work is to decrease the detection threshold and the time detection (number of periods), while maintaining a high level of robustness with respect to other unknown inputs. OFC with amplitude greater than the detection threshold should be detectable.

In addition, in order to ensure A/C safety and reliability, an important requirement is that the false alarm rate must be minimal. Indeed, after detection and confirmation of a failure event, the actuator concerned by the OFC detection is automatically reverting in passive mode. Control surfaces concerned by OFC detection are generally controlled by two actuators [12]: one assumes the control law (active actuator) and a redundant actuator (passive actuator) is in a stand-by mode and follows the movement of the active one. If a false alarm is triggered, there is a hand-over between both actuators (system reconfiguration) and then the redundancy on the concerned control surface is degraded. The non detection probability should also be minimal, because even if OFC are very improbable, the consequences are that extreme loads can be generated damaging the structure.

III. In-service OFC detection for A380

An analytical redundancy-based approach is applied to detect OFC on A380. The overall methodology is described in [12]. In the following section, we describe first the hydraulic actuator model used [12]. Next, the on boarded A380 solution is briefly presented.

A. *Hydraulic actuator modelling*

The nonlinear model is based on the physical behavior of the hydraulic actuator. The corresponding equation gives the actuator rod speed as a function of the hydraulic pressure delivered to the actuator and the forces applying on the control surface and reacted by the actuator. The actuator rod speed can be expressed as the rod speed command, weighted by two main contributor factors which are aerodynamics forces and the servocontrol load in damping mode (of the passive actuator in the case of two actuators). The actuator rod speed for a hydraulic servo control is expressed as:

$$\dot{y}(t) = V_0(t).\sqrt{\frac{\Delta P(t) - \dfrac{F_{aero}(t) + F_{damping}(t)}{S}}{\Delta P_{ref}}} \qquad (1)$$

where:

- $\Delta P(t)$ is the hydraulic pressure delivered to the actuator.
- $F_{aero}(t)$ represents the aerodynamic forces applying on the control surface. The corresponding model will not be detailed here as it is not of primary interest in this work.
- $F_{damping}(t)$ represents the servocontrol load of the adjacent actuator in damping mode:

$$F_{damping}(t) = K_a(t).\dot{y}(t)^2 \qquad (2)$$

- $K_a(t)$ is the actuator damping coefficient and $\dot{y}(t)$ represents the rod speed.
- S is the actuator piston surface area.
- ΔP_{ref} is the differential pressure corresponding to the maximum rod speed. This speed is reached when the servovalve is fully opened, i.e. when $\Delta P(t)=\Delta P_{ref}$ and when no opposed forces apply.
- $V_0(t)$ is the rod speed computed by the flight control computer. It corresponds to the maximal speed of one actuator alone with no load:

$$V_0(t) = K_{ci}K.(u(t) - y(t)) \qquad (3)$$

- K is the servo control gain and an estimated current $i(t)=K(u(t)-y(t))$ expressed in milliamp (servo-loop current derived from the flight control law order) is converted in rod speed $V_0(t)$ by a slope gain K_{ci}.

Equation (1) can also be written as the following continuous-time state space representation:

$$\begin{cases} \dot{x}(t) = \phi(x,u,\theta) \\ y(t) = x(t) \end{cases} \qquad (4)$$

where:

$$\phi(x,u,\theta) = K_{ci}K.(u(t)-x(t))\left(\frac{\theta_1(t)-\frac{\theta_2(t)}{S}}{\Delta P_{ref}+\frac{\theta_3(t)\left(K_{ci}K.(u(t)-x(t))\right)^2}{S}}\right)^{\frac{1}{2}} \quad (5)$$

where $\theta_1(t)= \Delta P(t)$, $\theta_2(t)= F_{aero}(t)$ and $\theta_3(t)= K_a(t)$.

Different saturations (actuator limit positions, maximum orders…) are taken into account in the varying gains (K_{ci}…).

B. A380 OFC detection

To the best of our knowledge, it is probably the first time that the concept of analytical redundancy is implemented on board for a family of civil aircraft for the detection of actuator failures on such a large number of control surfaces (3 pairs of ailerons, 2 pairs of elevators and two rudders on the A380). The fault indicating signal is the difference between the measured control surface position and the estimated position. The nonlinear hydraulic actuator model described above is used to estimate the position.

The overall method consists in two steps: residual generation and residual evaluation. Firstly, it consists in generating a residual by comparing the real position y of the control surface delivered by a sensor with an estimated position produced by the actuator model. The input of the model is the flight control law (the command used in the servo-control of the control surface). Secondly, the residual is decomposed in several spectral sub-bands [12]. As the computing resource is limited in the computer, the OFC detection is performed by counting oscillations directly on the filtered residual, in each subband. This consists in counting successive and alternate crossings of a given threshold. The failure amplitude that is detectable depends on the model quality. In this approach, the flight control law is considered as fault-free. All its oscillations are correct and are calculated in order to compensate perturbations (e.g. external disturbance such as turbulence). The hypothesis of a fault-free command is justified because the flight control law is also monitored by dedicated techniques.

C. Application to real flight data

In order to reduce the computational burden, K_a and ΔP are assumed to keep constant values (their most probable value) and F_{aero} is considered to be equal to zero. Such a simplification is justified on the A380 because it has been validated that the overall method permits the load requirements to be met for this A/C. In fact, these three parameters could be estimated from mathematical relationships using other measured parameters (e.g. slats and flaps configuration, speed, temperature…). However the loss of a measurement could make obsolete the whole detection strategy. Moreover, K_a and ΔP depend on varying operational conditions such as hydraulic fluid temperature or number of servo-control used simultaneously, which make their estimation process difficult.

The above detection technique has been validated during severe simulation campaigns on desktop simulators and industrial flight simulators. The robustness has been tested on the same test facilities and additionally during several hundred flight test hours on four A380 A/C.

The following figures show an example of results obtained during a real A380 flight, for the left inboard elevator. These figures show the dependency of the residual amplitude in function of the control law dynamic. When the dynamic of the flight control law is rapidly changing, the residual energy content becomes more important.

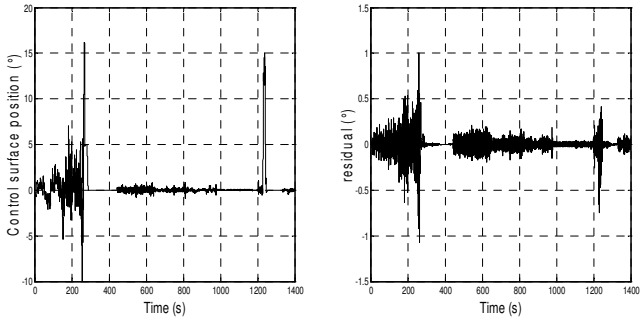

Fig. 2: a) actuator position (°) and b) the corresponding residual

In this example no OFC signal appears during the flight. Fig. 2.b shows an increasing of residual power when high control law dynamic appears. One can note that, during the first 300 seconds of the test scenario, the residual amplitude is often greater than 0.3°. Consequently detection threshold cannot be fixed to 0.3° because a lot of false alarm would appear during this period. Moreover, during the period between 500 and 1000 seconds the residual amplitude overflows regularly 0.2° due to the poor model quality.

IV. Joint Parameter and State Estimation

As already mentioned the OFC detection strategy described in the previous section has been intensively tested by Airbus, validated and certified for on-board implementation in the FCC and provides a complete OFC coverage without false alarm.

However, for upcoming and future Airbus programs, it could become necessary to improve the detection performance in case of more stringent requirements that would lead to the monitoring of OFC with smaller amplitude in less time of confirmation. But it appears that a reduction of residual power, particularly in dynamically changing stages, is necessary to detect less important OFC signals. Such OFC signals may go undetected if the modeling process is not sufficiently robust against neglected dynamics and parametric variations. The solution chosen in this work is to determine a more accurate actuator model, followed by the same decision making rule. This is done by estimating jointly state (actuator position) and the varying parameters K_a and F_{aero}. The estimated parameters are to be updated at each FCC sampling time.

Remark. Coming back to the model (5), it can be seen that

the parameters θ_1 and θ_2 cannot be identified in a unique way (structural identifiability). One solution would be to modify the structure of the physical model (5) to get an identifiable model structure, this can be done for example by replacing the term modeling F_{aero} by a polynomial function of the output. In this work ΔP has been fixed to a constant value, as a sensitivity analysis has shown that ΔP variations influence weakly the model output compared to F_{aero}.

To start, let the observed output y be decomposed as:

$$y = \hat{y} + \delta y \tag{6}$$

where $\hat{y}$ is the model output (estimated actuator position), and δy is a general error term resulting from the approximation of y by $\hat{y}$ (i.e. the part of the data which is not explained by the model). δy represents a general stochastic input that accounts for the combined effects of other factors affecting the original time series, such as noise, other stochastic inputs or model limitations.

Now, the relation (5) can be rewritten as an augmented nonlinear discrete-time state space representation, where the augmented state vector x contains actuator position output $\hat{y}$ as well as the varying parameters $\theta_i(k)$. This representation can be written as:

$$x(k+1) = f(x(k), u(k), v(k), \theta(k)) \tag{7}$$

$$y(k) = g(x(k), w(k), \theta(k)) \tag{8}$$

where f et g are known nonlinear functions, obtained from the basic equation (5) and k is the discrete time. Here, w is the measurement noise (dimension 1) and v is the process noise. The dimension of v is set to be 4.

The first 2 components of v allow for parametric variations, each parameter being modeled by a dynamic equation as:

$$\theta_i(k+1) = \theta_i(k) + v_i(k) \quad i = 1,2 \tag{9}$$

The third component of v affects the control input (u). The last one will affect, additively, the whole state equation. The latter can be seen as an additional degree of freedom which can be used to take into account the ageing of the actuator. Indeed, the structure of the state space model could evolve slightly with time, despite ground-based maintenance for actuator health monitoring.

v and w are both stationary white noise sequences, Gaussian with covariance matrices noted Q and R:

$$Q = E\left\{v(k)v(k)^T\right\} \text{ et } R = E\left\{w(k)w(k)^T\right\} \tag{10}$$

The initial estimates of state and covariance matrix are:

$$\bar{x}_0 = E\{x_0\} \tag{11}$$

$$P_0 = E\left\{(x_0 - \bar{x}_0)(x_0 - \bar{x}_0)^T\right\} \tag{12}$$

The a priori state and covariance estimates are obtained as the conditional expectation [22]:

$$\begin{aligned} \bar{x}_k &= E\left\{y_k \middle| Y^{k-1}\right\} \\ \bar{P}_k &= E\left\{(x_k - \bar{x}_k)(x_k - \bar{x}_k) \middle| Y^{k-1}\right\} \\ Y^{k-1} &= [y_0 \; y_1 \cdots y_{k-1}] \end{aligned} \tag{13}$$

The problem of recursively estimating state can be formulated as a nonlinear filtering problem [15]. According to a specification of the uncertainties in model and measurements, the filter calculates an optimal estimation of the augmented state and its covariance matrix. A classical way to solve the filtering equations is to use the Extended Kalman Filter (EKF) [15]. The filter has been widely used in the context of estimating the state and the parameters. The practical problems with the EKF are well-known, even when the hyper-parameters (Q and R) are well tuned. The EKF involves the integration of $n+n(n+1)/2$ (see [22] page 134) coupled differential equations. Moreover, it is well known that the parameter estimates can converge slower than the state estimates and in general, only local convergence can be expected [16]. In [17], the authors proposed a method based on polynomial approximation of the nonlinear approximations obtained with a multi-dimensional extension of Stirling's interpolation formula. In contrast to Taylor's formula, no derivatives are needed in the interpolation formula, only functions evaluations. This accommodates easy implementation and it is not necessary to assume differentiability of the nonlinear mappings. The method was judged suitable and superior to the EKF in a wide range of applications; see for instance [18].

To avoid duplicating materials from [17], the mechanization equations of the estimator are not given here, the interested reader can refer to [17] for further details. To obtain correct results, the tuning of Q and R is a crucial issue. By choosing values for the diagonal elements of the matrix Q, the flexibility of the model is controlled by the amount of noise allowed. Similarly, the matrix R controls the flexibility of the measurement equation. In this study, the optimization of the hyper parameters is done by iteratively testing different values and evaluating the results over a test period. The knowledge of maximum and minimum parameters bounds are helpful to set up initial covariance matrices (not given here for evident confidential reasons).

Again, all the saturations (maximum order, maximum actuator position…) are taken into account for the filter coding. Three different state space equations (7) have been used for the filter determination. These three non linear functions (f_1, f_2 and f_3) are used alternately according to (u-y) value and take into account the double slope gain transformation K_{ci} and the saturation model.

V. Simulation Results: Assessment of Performance and Robustness

A. Nominal case

Simulations have been run with the same flight data, as in section III.C. The following figures show an example (K_a) of the normalized estimated parameters and the residual obtained with the above estimation technique for the A380 hydraulic left inboard elevator.

Three different phases can be distinguished in Fig. 3.a). Initially, the parameter value is close to its initialised value, an important amplitude variation is observed between 100

and 250 seconds corresponding to an important control law dynamic (-10°/+15°). Finally, a last variation appears at 1200 seconds for a new control law dynamic variation (15°).

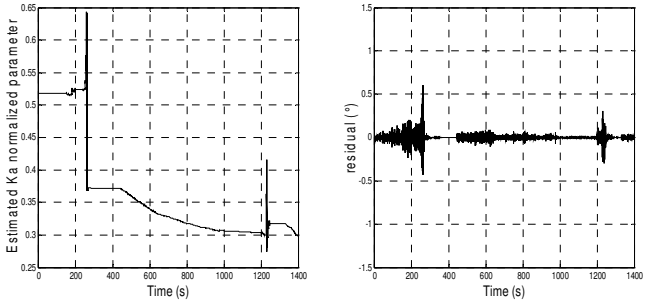

Fig. 3: *a*) Behavior of the estimated normalized parameter K_a *b*) Residual obtained with the nonlinear filter

Now, recall that the main motivation of this work was to get residuals that allow us to detect OFC with lower amplitude. In this way, the process would permit to decrease the threshold detection and smaller OFC signals could be detected. In the following, the method described in section III (Airbus technique) will be noted "Method 1" and the proposed technique presented in section IV will be referred to "Method 2". As the decision making process is the same for both methods (see section III.B), the detection performance will depend on the model quality. To compare the model quality, two time domain performance indicators and four frequency-domain distances are computed:

- *Time domain indicators*

The coefficient of determination (R^2) is an intuitively attractive indication of model accuracy since it indicates how much of the variability in the observed data is being reproduced by the model. Another useful indicator is the "Absolute Mean Error" (AME). The numerical results are:

	Method 1	Method 2
AME (°)	0.0316	0.0128
R^2	0.1220	0.023

Table 1: Performance time indicators

- *Frequency domain distances*

Four spectral distances have been computed between the Power Spectral Densities (PSD) of the real data and the PSD of the data produced by Method 1 and Method 2: the logarithmic distance (d_2), the Itakura-Saïto distance (d_{IS}), the cepstrum distance (d_c^2) and the Yegnanarayana distance (d_L^2).To save place and to avoid duplicating materials from [19], the mathematical definitions of these indicators are omitted here. The interested reader can refer to [19] for further details. In order to ease the comparison, these distances have been normalised with respect to Method 1. The results are given in Table 2.

	Method 1	Method 2
d_2	1	0.638
d_{IS}	1	0.077
d_c^2	1	0.638
d_L^2	1	0.644

Table 2: Spectral distances as performance indicators

One can see that all performance indicators are better for Method 2. The frequency domain distances clearly show that the distance between the real position and the position estimated with Method 2 is smaller than with Method 1, reinforcing the results presented in Table 1.

A quick comparison between Fig. 2.b (Method 1) and Fig. 3.b (Method 2) allows us to get a deeper insight into the situation. First, one can observe that at time 300 seconds (high dynamic behaviour of the control law, see Fig. 2.a), the corresponding residual amplitude is about 1° (Method 1, Fig. 2.b) and 0.6° (Method 2, Fig. 3.b). The residual amplitude variation is decreased when the Method 2 is used for the modelling stage. A second interesting feature is what happens between 500 and 1000 seconds. During this period, where the actuator has lower frequency dynamic (weak dynamic of the control law), the residual variations belong to the range [-0.2°, 0.2°] (Method 1, Fig. 2.b) and [-0.15°, 0.15°] (Method 2, Fig. 3.b).

Finally, the output of the decision rule for detecting OFC events (see section III) is analysed. The procedure consists in counting successive and alternate crossings of a given threshold. To avoid cumulating transitory threshold crossings (due to model uncertainties) that would necessarily lead to a false alarm, the oscillation counter is decremented after a given time (see [12]). Another reason to decrease the counter is that detection of oscillations is not required below a given frequency (see section II).

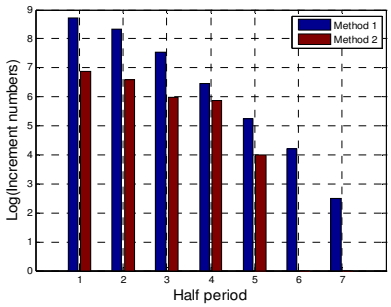

Fig. 4: Decision making for a threshold equal to 0.25°

Fig.4 shows the results for the decision making, when the threshold is fixed to a very small value (0.25°). This table shows the total number of increments for each value of the OFC counter. The detection performance is not the same for both methods. Here, the number of periods for OFC detection is fixed to 3 (6 half periods in the table).

Several false alarms occur with Method 1 whereas no false alarm appears with Method 2 for this threshold. This suggests that false alarm rate could be significantly reduced if the Method 2 is applied for the modelling stage. This simulation result shows clearly the benefit of the Method 2 if a small detection threshold is required.

The first objective (lower false alarm rate in nominal case with a small threshold) is then achieved; it is now important to verify that OFC signals could be detected successfully.

B. Failure cases

A simulated OFC with amplitude 0.4° and frequency 5 Hz

is injected at time 800 seconds. One can see that OFC signal is clearly exhibited with both methods (Fig. 5).

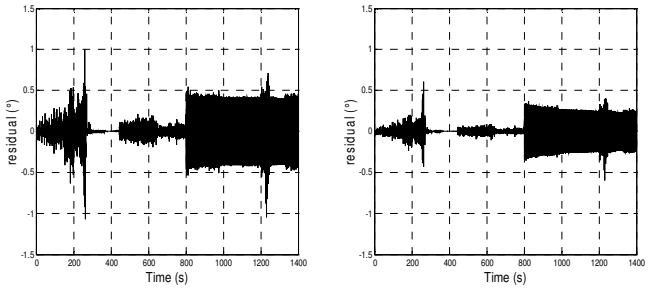

Fig. 5: Method1 and Method 2: faulty situation (liquid failure)

Fig.6 shows that with Method 1 (dashed line) and Method 2 (full line) the OFC detection (amplitude 0.4°) with a threshold fixed to 0.25° is succeeded. The time detection for Method 1 is 0.719s and for Method 2 is decreased to 0.703s.

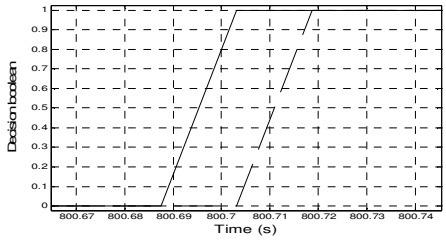

Fig. 6: OFC detection for 'liquid' OFC

These results show that with method 2 it is not possible to detect OFC smaller than 0.4° (with this threshold) because OFC signal is reduced on the residual by the methodology (Fig. 5.b). For this example, with a threshold of 0.25°, the benefit of method 2 is clear because no OFC false alarm appears. Further work is needed to estimate the observed attenuation and consequently the threshold to apply for a given level to detect. For this example no false alarms appear with Method 2 and the detection is performed slightly more rapidly than with Method 1.

VI. Conclusion

The problem studied is that of designing robust detection unit for early detection of OFC events that can occur in EFCS of civil A/C. It was shown that the nonlinear estimation techniques could be useful to significantly improve the quality of the actuator model. The simulation results suggest that OFC with less important amplitude can be successfully detected by the new strategy without degrading the robustness. A number of appealing avenues can be considered for further investigations. This study has focused on hydraulic actuators. Further investigations are necessary for to set up a systematic modeling process for the new generation actuators (EHA, EBHA) which are used on A380. Next, the whole procedure should be tested on dedicated industrial flight simulators, to assess the level of achievable detection performance and the associated computational burden. This is the topic of future works.

Acknowledgment

The financial support by "Airbus France Toulouse" is gratefully acknowledged.

References

[1] Jones H. L., Failure detection in linear systems Ph.D. dissertation, Dep. Aero. and Astro. Mass. Inst. Technol., Cambridge, MA. 1973.

[2] Beard R.V. Failure Accomodation in Linear System through Self-Reorganization. PhD thesis, Massachussets Inst. of Technology, 1971.

[3] Zolghadri A., Goetz C., Bergeon B. and Denoise X. Integrity monitoring of flight parameters using analytical redundancy. In UKACC International Conference on Control (CONTROL'98), pp. 1534-1539. Swansea, UK. 1998.

[4] Chen J., Patton R. Robust model-based fault diagnosis for dynamic systems. Kluwer Academic Publisher. 1999.

[5] Frank P., Ding S., Köppen-Seliger B. Current developments in the theory of FDI. Proceedings of SAFEPROCESS'2000, Budapest.

[6] Mangoubi, R.S. (1998). Robust estimation and failure detection: A concise treatment. Springer Verlag.

[7] Henry D., A. Zolghadri (2005). Design of Fault Diagnosis Filters: A Multi-Objective Approach. Journal of the Franklin Institute. Volume 342, Issue 4, July, Pages 421-446.

[8] Henry D., A. Zolghadri (2005). Design and analysis of robust FDI filters for uncertain systems under feedback control. Automatica, Volume 41, Issue 2, February, Pages 251-264.

[9] Frank P.M. Fault diagnosis in dynamic systems using analytical and knowledge-based redundancy: A survey and some new results. In Automatica, volume 26, issue 3, pp. 459-474. 1990.

[10] Zolghadri A. (2002). Early warning and prediction of flight parameter abnormalities for improved system safety assessment. Reliability Engineering and System Safety, vol. 16, pp 19-27.

[11] Zolghadri A. (2000). A redundancy-based strategy for safety management in a modern civil aircraft. Control Engineering Practice, Vol. 8, N° 5, pp 545-554.

[12] Goupil P. Oscillatory Failure Case detection in A380 Electrical Flight Control System by analytical redundancy. 17th IFAC Symposium on Automatic Control in Aerospace. Toulouse. France. 2007.

[13] Frank, P.M. and Ding, S.,X. (1997). Survey of robust residual generation and evaluation methods in observer-based fault detection systems. International journal of process control, 7(6), pp. 403-424.

[14] Zolghadri A, F. Castang, D. Henry (2006). Design of robust fault detection filters for multivariable feedback systems. International journal of modelling and simulation. ACTA Press, Vol. 26, N° 1.

[15] Ljung L. Söderstrôm T. Theory and practice of recursive identification. MIT PRESS, Cambridge, Mass. 1983.

[16] Reif, K., R. Unbehauen. The extended kalman filter as an exponential observer for nonlinear systems. IEEE Transactions on Signal Processing, 1999, 47(8), 2324-2328.

[17] Nogaard M., Ravn, O., Poulsen, N. New developments in state estimation for nonlinear systems. Automatica 2000, 36,1627-1638.

[18] Zolghadri A., M. Monsion, D. Henry, C. Marcionini, O. Petrique. Development of an operational model-based warning system for tropospheric ozone concentrations in Bordeaux, France. Environmental Modelling and Software, 2004, 19, 369-382.

[19] Basseville, M., Distance measures for signal processing and pattern recognition. European Journal Signal Processing, vol.18, no 4, Dec. 1989, pp.349-369.

[20] Traverse, P., I. Lacaze and J. Souyris (2004). Airbus Fly-By-Wire: A Total Approach To Dependability. Proc. 18th IFIP World Computer Congress, Toulouse, France, pp.191-212.

[21] Favre, C. (1994). Fly-by-wire for commercial aircraft: the Airbus experience. International Journal of Control, 59(1), 139-157.

[22] Lin C.F. Modern Navigation, guidance, and control processing. Vol II. PTR Prentice Hall, New Jersey. 1991.

[23] Brière B, C. Favre and P. Traverse (1995). A familly of fault-tolerant systems: electrical flight controls, from A320/330/340 to future military transport aircraft. Micoprocessors and Microsystems, Vol 19.

[24] Giesseler H. G. and H. M. Besch, "The oscillatory failure identification system (ofis)," in 36th AIAAS/ASME/ASCE/AHS/ASC Structures, structural dynamics and Material Conference, AIAA, Ed. New Orleans: AIAA/ASME, April 1995, pp. 3304–3317.

[25] Hou M. Amplitude and Frequency Estimator of a Sinusoid. IEEE Transactions on automatic control, Processing 2005, 50(6), 855-858.